

Dynamical quantum phase transitions: Role of topological nodes in wavefunction overlaps

Zhoushen Huang¹ and Alexander V. Balatsky^{1,2}

¹*Institute for Materials Science, Los Alamos National Laboratory, Los Alamos, NM 87545, USA**

²*NORDITA, Roslagstullsbacken 23, SE-106 91 Stockholm, Sweden[†]*

(Dated: June 23, 2018)

A sudden quantum quench of a Bloch band from one topological phase toward another has been shown to exhibit an intimate connection with the notion of a dynamical quantum phase transition (DQPT), where the returning probability of the quenched state to the initial state—i.e. the Loschmidt echo—vanishes at critical times $\{t^*\}$. Analytical results so far are limited to two-band models, leaving the exact relation between topology and DQPT unclear. In this work, we show that for a general multi-band system, a robust DQPT relies on the existence of nodes (i.e. zeros) in the wavefunction overlap between the initial band and the post-quench energy eigenstates. These nodes are topologically protected if the two participating wavefunctions have distinctive topological indices. We demonstrate these ideas in detail for both one and two spatial dimensions using a three-band generalized Hofstadter model. We also discuss possible experimental observations.

Introduction Advances in experimental techniques, in particular in cold atom systems [1–3], have reinvigorated recent interest in quantum dynamics [4]. A paradigmatic setup in this context is a quantum quench [5–9], wherein a system is prepared as an eigenstate $|\Psi\rangle$ of an initial Hamiltonian H_I , but evolved under a different Hamiltonian H_F . In a slow ramp [10, 11], one has in addition the control over how fast the switching between H_I and H_F can be, as well as what path to take in the space of Hamiltonians. Since $|\Psi\rangle$ typically consists of many excited states of H_F with a non-thermal distribution, its time evolution provides a unique venue for investigating issues in nonequilibrium quantum statistical mechanics such as thermalization, equilibration, or the lack thereof [4, 12–16]. A particularly fruitful approach to understanding dynamics after a quantum quench is by exploiting the formal similarity between the time evolution operator $\exp(-iHt)$, and the thermal density operator $\exp(-\beta H)$. This enables one to leverage and extend notions in equilibrium statistical mechanics to the realm of quantum dynamics. In this spirit, the return amplitude

$$G(t) = \langle \Psi | e^{-iH_F t} | \Psi \rangle = \sum_n \left| \langle \Phi^{(n)} | \Psi \rangle \right|^2 e^{-iE_n t} \quad (1)$$

can be thought of as a partition function along imaginary temperature $\beta = it$, with the prepared state $|\Psi\rangle$ as a fixed boundary [17]. Here $|\Phi^{(n)}\rangle$ and E_n are eigenstates and eigenvalues of the post-quench H_F , respectively. Heyl *et al* showed [18] that analogous to the thermal free energy, a dynamical free energy density [19] can be defined, $f(t) = -\log G(t)/L$, where L is system size. Singularities in f then signifies the onset of what was proposed as a *dynamical quantum phase transition* (DQPT). In statistical mechanics, phase transitions are closely related to the zeros of the partition function—known as Fisher zeros—in the complex temperature plane [20]. Historically, Yang and Lee were the first to connect phase transitions with zeros of the partition function in complexified parameter

space [21]. While Fisher zeros are always complex for finite systems, they may coalesce into a continuum (line in one parameter dimension, area in two parameter dimensions, etc) that cuts through the real temperature axis in the thermodynamic limit, giving rise to an equilibrium phase transition. Investigations on DQPT have followed a similar route by first solving the Fisher zeros in the complex temperature plane, and then identifying conditions for them to cross the axis of imaginary temperature (real time). DQPT is thus mathematically identified as $G(t^*) = 0$ at critical time(s) t^* [22]. DQPTs occur in both integrable [18, 23–30] and non-integrable [19, 31–34] spin systems for quenches across quantum critical points. They can further be classified by discontinuities in different orders of time derivatives of $f(t)$ [27, 35] *vis-a-vis* their thermal counterparts. Very recently DQPTs have also been shown to constitute *unstable* fixed points in the renormalization group flow, and are therefore subject to the notion of universality class and scaling [36].

Physically, the return amplitude $G(t)$ is related to the power spectrum of work performed during a quench, $G(\omega) = \sum_n \left| \langle \Phi^{(n)} | \Psi \rangle \right|^2 \delta(\omega - (E_n - E_I))$, which is the Fourier transform of $G(t)e^{-iE_I t}$, and E_I is the energy of the initial state [37–40]. This in principle makes $G(t)$, and hence DQPT, a measurable phenomenon. A practically more viable route to experimental verification is through measuring time evolution of thermodynamic quantities, which may exhibit post-quench oscillations at a time scale commensurate with the DQPT critical time t^* , and universal scaling near t^* [41]. In band systems, as we will show, they may also be identified by a complete depletion at t^* of sublattice or spin-polarized particle density at certain crystal momenta, see Eq. 8.

Parallel to the development of DQPT as the dynamical analogue of equilibrium phase transitions is the investigation on its relation with topology [24–27]. This issue arises naturally because in the transverse field Ising model, in which DQPT was first discovered, the quantum

critical point can be mapped to a topological phase transition at which the quantized Berry phase of the *fermionized* Hamiltonian jumps between 0 and π . DQPT in this two-band fermion model was attributed to the occurrence of “population inversion” [18] where it becomes equally probable to find the initial state in either of the two post-quench bands, a consequence of the Berry phase jump [26]. The same analysis has been extended to various two-band models in one- and two-spatial dimensions (1D/2D) [25–29], where definitive connection was found between DQPT and quench across topological transitions, although some complications exist [42]. DQPTs have also been demonstrated for quenches within the same topological phase [24, 25, 33], although from the point of view of topological protection, these are not robust as they require fine-tuning of the Hamiltonians.

The purpose of this work is to develop a general theory *beyond two band models* to clarify the relation between *robust* DQPT and topology. We will show that a robust DQPT—one which is insensitive to the details of the pre- and post-quench Hamiltonians other than the phases to which they belong—relies on the existence of zeros (or nodes) in the wavefunction overlap between the initial band and all eigenstates of the post-quench Hamiltonian. These nodes are topologically protected if the two participating wavefunctions have distinctive topological indices: for example, the Chern number difference $|C_\psi - C_\phi|$ provides a lower bound to the number of \mathbf{k} -space nodes in the overlap $\langle \phi_{\mathbf{k}} | \psi_{\mathbf{k}} \rangle$, see Theorem 1. These considerations lead to the notion of *topological* and *symmetry-protected DQPTs* which we will demonstrate in detail using a 3-band generalized Hofstadter model. Analysis of a 1D 3-band model exhibiting symmetry-protected DQPT can be found in Supplemental Materials (SM).

Amplitude and phase conditions of DQPT The DQPT condition $G(t^*) = 0$ can be interpreted geometrically as the complex numbers $z_n(t) = |\langle \Phi^{(n)} | \Psi \rangle|^2 e^{-iE_n t}$ forming a closed polygon in the complex plane at t^* , see Fig. 1. The time-independent content of this observation is that the amplitudes $\{|z_n|\}$ satisfy a generalized triangle inequality, $\sum_{m \neq n} |z_m| \geq |z_n| \forall n$. Invoking $\langle \Psi | \Psi \rangle = \sum_n |z_n| = 1$, one has the *amplitude condition*,

$$|z_n| = \left| \langle \Phi^{(n)} | \Psi \rangle \right|^2 \stackrel{!}{\leq} \frac{1}{2} \quad \forall n. \quad (2)$$

For $\{|z_n|\}$ that satisfy Eq. 2, solutions to $\sum_n |z_n| e^{-i\varphi_n} = 0$ exist and form a subspace $\mathcal{M}_{\{|z_n|\}}$ on the N -torus,

$$\mathcal{M}_{\{|z_n|\}} \in \mathcal{T}^N : \left\{ \{e^{-i\varphi_n}\} \left| \sum_{n=1}^N |z_n| e^{-i\varphi_n} = 0 \right. \right\}. \quad (3)$$

To set off DQPT, the dynamical phases must be able to evolve into $\mathcal{M}_{\{|z_n|\}}$. This constitutes the *phase condition*,

$$\exists t^* : \{e^{-iE_n t^*}\} \in \mathcal{M}_{\{|z_n|\}}. \quad (4)$$

DQPT requires both conditions to hold simultaneously.

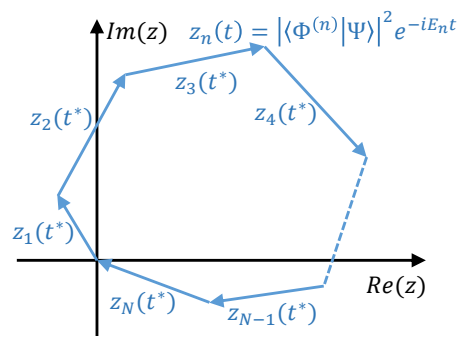


FIG. 1. (Color online) Geometric representation of the DQPT condition $G(t^*) = \sum_n z_n(t^*) = 0$. $\{z_n(t^*)\}$ must form a closed polygon in the complex plane, and hence satisfy a generalized triangle inequality $|z_n| \leq \sum_{m \neq n} |z_m|$. Wavefunction normalization $\langle \Psi | \Psi \rangle = \sum_n |z_n| = 1$ then leads to $|z_n| \leq \frac{1}{2}$.

Phase ergodicity in few-level systems At first glance, the phase condition may seem to be the more stringent one. After a quench across a quantum phase transition, a many-body initial state $|\Psi\rangle$ typically has overlap with an extensive amount of eigenstates of the post-quench Hamiltonian H_F and therefore the amplitudes $\langle \Phi^{(n)} | \Psi \rangle$ are generically exponentially small in system size, rendering Eq. 2 satisfied in general. Existence of DQPT then relies entirely on the phase condition. Integrable systems, however, point to the possibility that the amplitude and phase conditions may be intricately related and traded for one another. Such systems can effectively be broken down into few-level subsystems labeled by quantum numbers \mathbf{k} , say $N_{\mathbf{k}}$ levels $\{E_{\mathbf{k},n}\}$ for $n = 1, 2, \dots, N_{\mathbf{k}}$ in the \mathbf{k} sector. Correspondingly $G(t) = \prod_{\mathbf{k}} G(\mathbf{k}, t)$. For the transverse field Ising model, Kitaev’s honeycomb model [43], and band insulator models, \mathbf{k} is the Bloch momentum. It is known that as long as the $N_{\mathbf{k}} - 1$ gaps, $\Delta_{\mathbf{k},n} = E_{\mathbf{k},n+1} - E_{\mathbf{k},n}$, are not rationally related, the dynamical phases $\{e^{-iE_{\mathbf{k},n} t}\}$ are *ergodic* on the $N_{\mathbf{k}}$ -torus up to an overall phase [44], and *will* therefore evolve into its subspace $\mathcal{M}_{\{|z_n|\}}$ (Eq. 3). Phase ergodicity thus guarantees the phase condition Eq. 4, and DQPT in each \mathbf{k} sector depends entirely on the amplitude condition.

Robust DQPT protected by nodes in wavefunction overlap Hereafter, we focus on quenches in multi-band Bloch systems with N_B bands. For simplicity we use a single filled band $|\psi(\mathbf{k})\rangle$ as the pre-quench state. Generalization to multiple filled bands is straightforward. The post-quench return amplitude is $G(t) = \prod_{\mathbf{k}} G(\mathbf{k}, t)$,

$$G(\mathbf{k}, t) = \sum_{n=1}^{N_B} \left| \langle \phi^{(n)}(\mathbf{k}) | \psi(\mathbf{k}) \rangle \right|^2 e^{-i\varepsilon_n(\mathbf{k})t}, \quad (5)$$

where $|\phi^{(n)}(\mathbf{k})\rangle$ and $\varepsilon_n(\mathbf{k})$ are respectively the post-quench energy eigenstates and eigenvalues. *Assume phase ergodicity holds at all \mathbf{k} points*—this is a very relaxed requirement provided there is no degeneracy at any

\mathbf{k} point. Then DQPT amounts to the existence of at least one \mathbf{k} at which Eq. 2 is satisfied, namely

$$\exists \mathbf{k} \in \text{Brillouin Zone} : \left| \langle \phi^{(n)}(\mathbf{k}) | \psi(\mathbf{k}) \rangle \right|^2 \leq \frac{1}{2} \forall n. \quad (6)$$

We now discuss how Eq. 6 and hence DQPT can arise from nodes in wavefunction overlaps. Note that this is *not* the only way to get DQPT. Its virtue lies in its robustness against perturbations to the Hamiltonians. In SM, we provide examples where DQPTs with no overlap node can be easily avoided simply by Hamiltonian parameter tuning without crossing a phase boundary. The overlap nodes are, on the other hand, typically topologically protected, a point we will return to later. Now consider the following quench. Let $a = 1, 2, \dots, N_B$ label “sublattices”, which in general may also include other degrees of freedom, e.g., orbitals, spins, etc. Prepare the pre-quench state by filling $a = 1$,

$$|\Psi\rangle = \prod_{\mathbf{r}} \psi_{\mathbf{r},1}^\dagger |\emptyset\rangle = \prod_{\mathbf{k}} \psi_{\mathbf{k},1}^\dagger |\emptyset\rangle, \quad (7)$$

where $\psi_{\mathbf{r},a}^\dagger$ creates an electron on sublattice a in unit cell \mathbf{r} , $|\emptyset\rangle$ is the vacuum, $\psi_{\mathbf{k},a}^\dagger = \frac{1}{\sqrt{N}} \sum_{\mathbf{r}} e^{i\mathbf{k}\cdot\mathbf{r}} \psi_{\mathbf{r},a}^\dagger$, and N is the total number of unit cells. The system is then time-evolved under an integer quantum Hall Hamiltonian $\hat{H} = \sum_{\mathbf{k}} \hat{H}(\mathbf{k})$ where $\hat{H}(\mathbf{k}) = \sum_{a,b=1}^{N_B} H_{a,b}(\mathbf{k}) \psi_{\mathbf{k},a}^\dagger \psi_{\mathbf{k},b} = \sum_{n=1}^{N_B} \varepsilon_{\mathbf{k},n} \phi_{\mathbf{k},n}^\dagger \phi_{\mathbf{k},n}$, and we assume the Chern number of all bands of $\hat{H}(\mathbf{k})$ are non-zero, $C_n \neq 0 \forall n$. The overlap in Eq. 6 is $\langle \emptyset | \phi_{\mathbf{k},n} \psi_{\mathbf{k},1}^\dagger | \emptyset \rangle = \phi_1^{(n)}(\mathbf{k})^*$, where $\phi_a^{(n)}(\mathbf{k}) = \langle a | \phi^{(n)}(\mathbf{k}) \rangle$ is the a^{th} component of $|\phi^{(n)}(\mathbf{k})\rangle = (\phi_1^{(n)}(\mathbf{k}), \phi_2^{(n)}(\mathbf{k}), \dots, \phi_{N_B}^{(n)}(\mathbf{k}))^t$, an eigenvector of the post-quench Hamiltonian matrix $H(\mathbf{k})$. It is known that any component $\phi_a^{(n)}(\mathbf{k}) \forall a$ must have *at least* $|C_n|$ zeros in the Brillouin zone [45], see also Thm. 1. Now assume at an arbitrary Bloch momentum \mathbf{k}_0 , $\phi_1^{(n_1)}$ has the highest weight: $|\phi_1^{(n_1)}(\mathbf{k}_0)| > |\phi_1^{(n \neq n_1)}(\mathbf{k}_0)|$. The existence of node means $\phi_1^{(n_1)}$ cannot remain as the highest weight element over the entire Brillouin zone, and hence must switch rank with the second highest weight element, say $\phi_1^{(n_2)}$, at some point \mathbf{k}_c : $|\phi_1^{(n_1)}(\mathbf{k}_c)| = |\phi_1^{(n_2)}(\mathbf{k}_c)| \geq |\phi_1^{(n \neq n_1, n_2)}(\mathbf{k}_c)|$ [46]. Together with the normalization $\langle \emptyset | \psi_{\mathbf{k},1}^\dagger \psi_{\mathbf{k},1} | \emptyset \rangle = \sum_n |\phi_1^{(n)}|^2 = 1$, one concludes that at $\mathbf{k} = \mathbf{k}_c$, Eq. 6 is satisfied.

Note that in this case, the return amplitude $G(\mathbf{k}, t)$ is related to the \mathbf{k} -space sublattice particle density,

$$\rho_{\mathbf{k},a}(t) \equiv \langle \Psi(t) | \psi_{\mathbf{k},a}^\dagger \psi_{\mathbf{k},a} | \Psi(t) \rangle = |G(\mathbf{k}, t)|^2. \quad (8)$$

A DQPT can thus be identified by $\rho_{\mathbf{k},a}(t^*) = 0$, i.e., a complete depletion of particles with momentum \mathbf{k} on sublattice a (or orbital, spin, etc.), which may be experimentally measurable.

The argument above for node-protected DQPT applies to any pre-/post-quench combinations. In general, if the

overlap of the pre-quench band $|\psi(\mathbf{k})\rangle$ with *every* eigenstate $|\phi^{(n)}(\mathbf{k})\rangle$ of $H_F(\mathbf{k})$ has nodes in the Brillouin zone, then the triangle inequality Eq. 6 is guaranteed, and a robust DQPT would occur. This criterion can be written in a form more amenable to numerical test,

$$\psi_{\text{MaxMin}} \equiv \max_n \left[\min_{\mathbf{k}} |\langle \phi^{(n)}(\mathbf{k}) | \psi(\mathbf{k}) \rangle| \right], \quad (9)$$

$$\psi_{\text{MaxMin}} = 0 \Leftrightarrow \text{Robust DQPT}. \quad (10)$$

Topological protection of nodes in wavefunction overlaps There is a curious connection between wavefunction zeros and quantization. In elementary quantum mechanics, nodes in the radial wavefunction is related to the principal quantum number [47]. In continuum integer quantum Hall systems, the number of nodes in the wavefunction $\psi(\mathbf{r}) = \langle \mathbf{r} | \psi \rangle$ for \mathbf{r} in a magnetic unit cell is given by its Chern number magnitude $|C|$ [45]. These nodes persist even in the presence of weak disorder [48]. On a lattice, $|C|$ gives the number of \mathbf{k} -space nodes in all wavefunction components $\psi_a(\mathbf{k}) = \langle a | \psi(\mathbf{k}) \rangle \forall a$ [45], a phenomenon closely related to the energetic spectral flow of the edge states [49]. Note that the relation between C and wavefunction nodes relies on one participant of the overlap, namely the basis states $|\mathbf{r}\rangle$ and $|a\rangle$, to be topologically trivial. If both participants can be nontrivial, the number of nodes in their overlap should depend on both topological indices on an equal footing. Indeed we have the following theorems,

Theorem 1 *In 2D, the overlap of Bloch bands $|\psi(\mathbf{k})\rangle$ and $|\phi(\mathbf{k})\rangle$, with Chern numbers C_ψ and C_ϕ respectively, must have at least $|C_\psi - C_\phi|$ nodes in the Brillouin zone.*

Theorem 2 *In 1D, the Berry phase γ of a real Bloch band, $|\psi(k)\rangle = (\psi_1(k), \psi_2(k), \dots)^t$, $\psi_a(k) \in \mathbb{R} \forall a$, is quantized to 0 or π . The overlap of two real bands $|\psi(k)\rangle$ and $|\phi(k)\rangle$, with Berry phases γ_ψ and γ_ϕ respectively, must have at least one node if $\gamma_\psi \neq \gamma_\phi$.*

See SM for proof. Note that symmetry protection may enforce a Hamiltonian to be real [50], leading to the real bands in Thm. 2. This prompts the notion of *symmetry-protected DQPT*, reminiscent of symmetry-protected topological phases that may be classified by topological numbers at high-symmetry hyper-surfaces [50–52]. An example will be given later, see also SM.

Generalized Hofstadter model We demonstrate ideas discussed above using a generalized Hofstadter model,

$$H(\mathbf{k}, t, m) = \begin{pmatrix} d_1 & v_1 & v_3 e^{ik_y} \\ v_1 & d_2 & v_2 \\ v_3 e^{-ik_y} & v_2 & d_3 \end{pmatrix}, \quad (11)$$

$$d_a = 2 \cos(k_x + a\varphi) + am,$$

$$v_a = 1 + 2t \cos \left[k_x + \left(a + \frac{1}{2} \right) \varphi \right],$$

$$a = 1, 2, 3, \quad \varphi = \frac{2\pi}{3}.$$

The nearest neighbor hopping is set as 1. At $t = m = 0$, we recover the Hofstadter model [49, 53–58] on a square lattice with magnetic flux φ per structural unit cell, and its magnetic unit cell consists of 3 structural unit cells along the y direction. $t \neq 0$ allows for second neighbor (i.e. diagonal) hopping, and $m \neq 0$ describes a flux-commensurate onsite sawtooth potential. See SM for phase diagram. At $k_y = 0$ and π , $H(\mathbf{k})$ is invariant under the combined transformation of time-reversal, $H(\mathbf{k}) \rightarrow H^*(-\mathbf{k})$, and inversion, $H(\mathbf{k}) \rightarrow H(-\mathbf{k})$, and is hence real. Eigenstates there are subject to Thm. 2.

Now consider quenches in which the initial state is prepared by filling one of the three bands of a pre-quench Hamiltonian parameterized by t_i, m_i , and evolved using a post-quench Hamiltonian with t_f, m_f [59]. In Fig. 2, we keep t_i, m_i, m_f fixed, and plot the MaxMin (Eq. 9) of the three pre-quench bands as functions of the post-quench t_f . By varying t_f , the post-quench $H(\mathbf{k})$ is swept through six different topological phases as labeled in Fig. 2.

Let us illustrate topological and symmetry-protected DQPTs with two examples, using $\psi^{(2)}$ as the pre-quench state (blue circled line in Fig. 2): (i) *Topological DQPT* protected by 2D Chern number. Consider the quench from $\psi^{(2)}$ to phase 5. In this case, the Chern number of the pre-quench state ($C = -1$) differs from all three Chern numbers of the post-quench Hamiltonian ($C = [1, -2, 1]$), thus from Thm. 1, all three overlaps have nodes, and Eq. 6 is satisfied. (ii) *Symmetry-protected DQPT*. Consider the quench from $\psi^{(2)}$ to phase 2. In this case, the pre-quench Chern number ($C = -1$) is identical to at least one of the post-quench Chern numbers ($C = [0, 1, -1]$), hence not all overlaps have nodes originating from Thm. 1. Nevertheless, at $k_y = 0$ and π where the Hamiltonian is real, its eigenstates can be classified by their Berry phases. One can find numerically that at $k_y = 0$, the Berry phase for $\psi^{(2)}$ is $\gamma = 0$, whereas that of the post-quench $\phi^{(3)}$ (the one with $C = -1$) is $\gamma = \pi$. According to Thm. 2, therefore, $\langle \phi^{(3)} | \psi^{(2)} \rangle_{k_y=0}(k_x)$ has node along k_x . Nodes in overlaps of $\psi^{(2)}$ with $\phi^{(1)}$ and $\phi^{(2)}$ are still protected by Thm. 1. Thus all three overlaps have nodes and DQPT is protected.

Details of all 18 quench types (3 pre-quench states \times 6 post-quench phases) can be found in SM. We should note here that out of all 18 types, 2 robust DQPTs ($\psi^{(1)}$ to phases 2 and 5) exhibit an even number of overlap nodes at $k_y = 0$ and/or π not accounted for by Thms. 1 and 2. By tuning $t_{i,f}$ and $m_{i,f}$, we were able to shift the nodes along k_x as well as to change the total number of nodes by an even number, but could not entirely eliminate them. We suspect however that they could eventually be eliminated in an enlarged parameter space.

Conclusion and discussion In this work, we showed that for quantum quenches between gapped phases in a generic multi-band system, a robust dynamical quantum phase transition (DQPT) is a consequence of momentum-space nodes (or zeros) in the wavefunction overlap be-

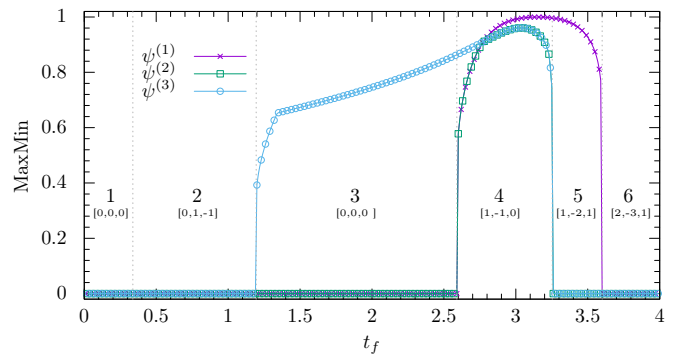


FIG. 2. (Color online) Plot of ψ_{MaxMin} (Eq. 9) as functions of the post-quench t . Pre-quench state is prepared by filling one of the three bands $\psi^{(1,2,3)}$ of the generalized Hofstadter model Eq. 11 with parameters $t_i = 3$ and $m_i = 2.8$. Post-quench $H(\mathbf{k})$ has fixed $m_f = 3$ and a varying t_f , sweeping it through six topological phases labeled by its three Chern numbers (ordered from lower to higher band). The pre-quench Hamiltonian is in phase 4. A robust DQPT can be identified by $\psi_{\text{MaxMin}} = 0$ (Eq. 10). Note that ψ_{MaxMin} changes between zero and non-zero only at phase boundaries, verifying robust DQPT as a feature of topological phases insensitive to parameter tuning. See SM for detailed account of all 18 types of quenches shown here.

tween the pre-quench state and all post-quench energy eigenstates. Nodes in wavefunction overlaps are topologically protected if the topological indices of the two participating wavefunctions—such as Chern number in 2D and Berry phase in 1D—are different.

Our main tenets here are the triangle inequality Eq. 6, and phase ergodicity. It is interesting to note that collapsing a band gap would affect both conditions: right at the gap collapsing point $\varepsilon_{\mathbf{k}}^{(n)} = \varepsilon_{\mathbf{k}}^{(n+1)}$, the two phases become mutually locked; as the gap re-opens, the system has gone through a topological transition, which changes the node structure in wavefunction overlaps. We also note that while the *existence* of topological and symmetry-protected DQPT is insensitive to details of the energy band structure, the exact times at which it would occur will inevitably depend on the latter. The shortest critical time will be upper-bounded by the recurrence time of the phases, which, for few-level systems such as band insulators, should remain physically relevant [60].

DQPT in band systems is in principle experimentally measurable. As shown in Eq. 8, DQPT can be identified as the depletion of “sublattice” particle density $\rho_{\mathbf{k},a}(t^*)$ where sublattice a can also refer to spin, orbital, etc. Particle density $\rho_{\mathbf{k}}(t) = \sum_a \rho_{\mathbf{k},a}(t)$ can already be measured in cold atom systems by time-of-flight experiments [1–3, 54, 61]. It is not hard to envisage an additional procedure of “sublattice” isolation in such measurements, e.g., by using a magnetic field for spin filtering, or by releasing other sublattices $b \neq a$ slightly earlier than a .

Acknowledgments We are grateful to D.P. Arovas, A. Alexandradinata, and A. Saxena for useful discussions. We thank J.M. Zhang for communication of a recent work [62]. Work at LANL was supported by the US DOE BES E304/E3B7. Work at NORDITA was supported by ERC DM 321031.

Note added Ref. [63] appeared shortly after the completion of this manuscript, where results regarding topological nodes in wavefunction overlaps, consistent with Theorems 1 and 2 presented here, are obtained elegantly by appealing to adiabatic continuity. In Ref. [64], topological nodes have also been connected to non-analyticity in physical observables upon tuning the post-quench Hamiltonian across a topological transition. We thank K. Sun and A. Das for communications.

* zsh@lanl.gov

† avb@nordita.org

- [1] I. Bloch, J. Dalibard, and W. Zwerger, *Rev. Mod. Phys.* **80**, 885 (2008).
- [2] I. Bloch, J. Dalibard, and S. Nascimbène, *Nature Physics* **8**, 267 (2012).
- [3] T. Langen, R. Geiger, and J. Schmiedmayer, *Annual Review of Condensed Matter Physics* **6**, 201 (2015), 1408.6377.
- [4] A. Polkovnikov, K. Sengupta, A. Silva, and M. Vengalattore, *Rev. Mod. Phys.* **83**, 863 (2011).
- [5] F. Iglói and H. Rieger, *Phys. Rev. Lett.* **85**, 3233 (2000).
- [6] E. Altman and A. Auerbach, *Phys. Rev. Lett.* **89**, 250404 (2002).
- [7] A. Polkovnikov, S. Sachdev, and S. M. Girvin, *Phys. Rev. A* **66**, 053607 (2002).
- [8] K. Sengupta, S. Powell, and S. Sachdev, *Phys. Rev. A* **69**, 053616 (2004).
- [9] P. Calabrese and J. Cardy, *Physical Review Letters* **96**, 136801 (2006), cond-mat/0601225.
- [10] R. Barankov and A. Polkovnikov, *Physical Review Letters* **101**, 076801 (2008), 0804.2894.
- [11] F. Pollmann, S. Mukerjee, A. G. Green, and J. E. Moore, *Phys. Rev. E* **81**, 020101 (2010).
- [12] R. Nandkishore and D. A. Huse, *Annual Review of Condensed Matter Physics* **6**, 15 (2015), 1404.0686.
- [13] J. Eisert, M. Friesdorf, and C. Gogolin, *Nature Physics* **11**, 124 (2015), 1408.5148.
- [14] L. D’Alessio, Y. Kafri, A. Polkovnikov, and M. Rigol, *ArXiv e-prints* (2015), 1509.06411.
- [15] F. H. L. Essler and M. Fagotti, *ArXiv e-prints* (2016), 1603.06452.
- [16] J. Millen and A. Xuereb, *New Journal of Physics* **18**, 011002 (2016), 1509.01086.
- [17] A. LeClair, G. Mussardo, H. Saleur, and S. Skorik, *Nuclear Physics B* **453**, 581 (1995), hep-th/9503227.
- [18] M. Heyl, A. Polkovnikov, and S. Kehrein, *Phys. Rev. Lett.* **110**, 135704 (2013).
- [19] M. Fagotti, *ArXiv e-prints* (2013), 1308.0277.
- [20] M. E. Fisher, *The Nature of Critical Points*, vol. 7 of *Lectures in Theoretical Physics* (the University of Colorado Press, 1965).
- [21] C. N. Yang and T. D. Lee, *Phys. Rev.* **87**, 404 (1952). T. D. Lee and C. N. Yang, *Physical Review* **87**, 410 (1952).
- [22] Note1, the formal similarity between e^{-iHt} and $e^{-\beta H}$ is routinely used in field theoretic calculations such as correlators, where the thermal and quantum-dynamic results are related through Wick rotation. Knowledge in one domain can then be transcribed into the other without additional calculation. This “equivalence”, however, relies on the existence of an analytic continuation between it and β in the complex temperature plane. The presence of closed and/or semi-infinite Fisher zero lines divides the complex temperature plane into disjoint regions, and the correspondence between it and β will break down if they reside in different regions. For quenches that exhibit DQPT, as pointed out in Ref. [18], this implies that non-equilibrium time evolution (i.e. along the imaginary temperature axis) is in general not governed by the equilibrium thermodynamics (along the real temperature axis).
- [23] B. Pozsgay, *Journal of Statistical Mechanics: Theory and Experiment* **10**, 10028 (2013), 1308.3087.
- [24] S. Vajna and B. Dóra, *Phys. Rev. B* **89**, 161105 (2014).
- [25] J. M. Hickey, S. Genway, and J. P. Garrahan, *Phys. Rev. B* **89**, 054301 (2014).
- [26] S. Vajna and B. Dóra, *Phys. Rev. B* **91**, 155127 (2015).
- [27] M. Schmitt and S. Kehrein, *Phys. Rev. B* **92**, 075114 (2015).
- [28] U. Divakaran, S. Sharma, and A. Dutta, *ArXiv e-prints* (2016), 1601.04851.
- [29] S. Sharma, U. Divakaran, A. Polkovnikov, and A. Dutta, *ArXiv e-prints* (2016), 1601.01637.
- [30] J. C. Budich and M. Heyl, *Phys. Rev. B* **93**, 085416 (2016).
- [31] C. Karrasch and D. Schuricht, *Phys. Rev. B* **87**, 195104 (2013).
- [32] J. N. Kriel, C. Karrasch, and S. Kehrein, *Phys. Rev. B* **90**, 125106 (2014).
- [33] F. Andraschko and J. Sirker, *Phys. Rev. B* **89**, 125120 (2014).
- [34] S. Sharma, S. Suzuki, and A. Dutta, *Phys. Rev. B* **92**, 104306 (2015).
- [35] E. Canovi, P. Werner, and M. Eckstein, *Phys. Rev. Lett.* **113**, 265702 (2014).
- [36] M. Heyl, *Phys. Rev. Lett.* **115**, 140602 (2015).
- [37] P. Talkner, E. Lutz, and P. Hänggi, *Phys. Rev. E* **75**, 050102 (2007), cond-mat/0703189.
- [38] M. Campisi, P. Hänggi, and P. Talkner, *Reviews of Modern Physics* **83**, 771 (2011), 1012.2268.
- [39] C. Jarzynski, *Phys. Rev. Lett.* **78**, 2690 (1997).
- [40] S. Deffner and A. Saxena, *Phys. Rev. E* **92**, 032137 (2015).
- [41] M. Heyl, *Phys. Rev. Lett.* **113**, 205701 (2014).
- [42] Note2, e.g., in 2D integer quantum Hall systems, DQPT is related to the change in the *absolute value* of Chern number $|C|$ instead of C [26].
- [43] A. Kitaev, *Annals of Physics* **321**, 2 (2006), cond-mat/0506438.
- [44] I. Cornfeld, A. Sossinskii, S. Fomin, and Y. Sinai, *Ergodic Theory* (Springer, 1982).
- [45] M. Kohmoto, *Annals of Physics* **160**, 343 (1985).
- [46] Note3, for two band models, \mathbf{k}_c is where the so-called “population inversion” occurs.
- [47] L. D. Landau and E. M. Lifshits, *Quantum Mechanics: Non-relativistic Theory* (Butterworth-Heinemann, 1977).

- [48] D. P. Arovas, R. N. Bhatt, F. D. M. Haldane, P. B. Littlewood, and R. Rammal, Phys. Rev. Lett. **60**, 619 (1988).
- [49] Y. Hatsugai, Phys. Rev. Lett. **71**, 3697 (1993).
- [50] C. Fang, Y. Chen, H.-Y. Kee, and L. Fu, Phys. Rev. B **92**, 081201 (2015), 1506.03449.
- [51] S. Ryu, A. P. Schnyder, A. Furusaki, and A. W. W. Ludwig, New Journal of Physics **12**, 065010 (2010), 0912.2157.
- [52] A. Alexandradinata, C. Fang, M. J. Gilbert, and B. A. Bernevig, Phys. Rev. Lett. **113**, 116403 (2014).
- [53] D. R. Hofstadter, Phys. Rev. B **14**, 2239 (1976).
- [54] E. Zhao, N. Bray-Ali, C. J. Williams, I. B. Spielman, and I. I. Satija, Phys. Rev. A **84**, 063629 (2011).
- [55] Z. Huang and D. P. Arovas, Phys. Rev. B **86**, 245109 (2012), 1201.0733.
- [56] L. Wang, A. A. Soluyanov, and M. Troyer, Physical Review Letters **110**, 166802 (2013), 1303.1061.
- [57] F. Harper, S. H. Simon, and R. Roy, Phys. Rev. B **90**, 075104 (2014), 1404.5303.
- [58] M. Aidelsburger, M. Lohse, C. Schweizer, M. Atala, J. T. Barreiro, S. Nascimbène, N. R. Cooper, I. Bloch, and N. Goldman, Nature Physics **11**, 162 (2015), 1407.4205.
- [59] Note4, an initial state of two filled bands is equivalent to one with a single filled band through particle-hole transformation.
- [60] Note5, under special circumstances, the DQPT critical time may also emerge at a much shorter time scale, e.g., the inverse level spacing, see Ref. [62].
- [61] D.-L. Deng, S.-T. Wang, and L.-M. Duan, Phys. Rev. A **90**, 041601 (2014).
- [62] J. M. Zhang and H.-T. Yang, ArXiv e-prints (2016), 1601.03569.
- [63] J. Gu and K. Sun, ArXiv e-prints (2016), 1605.07627.
- [64] S. Roy, R. Moessner, and A. Das, ArXiv e-prints (2016), 1606.06673.

SUPPLEMENTAL MATERIALS:

RELATION BETWEEN NODES IN WAVEFUNCTION OVERLAPS AND TOPOLOGICAL INDICES

In this section, we prove two theorems relating momentum-space nodes in wavefunction overlaps to the topological indices of the two participating wavefunctions.

Theorem 1 *In 2D, the overlap of two Bloch bands $|\psi(\mathbf{k})\rangle$ and $|\phi(\mathbf{k})\rangle$, with Chern numbers C_ψ and C_ϕ respectively, must have at least $|C_\psi - C_\phi|$ nodes in the Brillouin zone. If it has no node, $C_\psi = C_\phi$.*

Proof 1 Let us first prove the second part of the theorem, where $\langle\phi|\psi\rangle$ has no node. Here $|\psi(\mathbf{k})\rangle = (\psi_1(\mathbf{k}), \psi_2(\mathbf{k}), \dots)^T$ and $|\phi(\mathbf{k})\rangle = (\phi_1(\mathbf{k}), \phi_2(\mathbf{k}), \dots)^T$ are column vectors. Assume ϕ_1 , the first component of ϕ , has N_ϕ zeros in the Brillouin zone (BZ). Following Refs. 45 and 49, we partition the BZ into $N_\phi + 1$ regions $R_0, R_1, \dots, R_{N_\phi}$, where $R_{i>0}$ is an infinitesimal neighborhood of the i^{th} zero of ϕ_1 , and $R_0 = \text{BZ} \setminus (\cup_{i=1}^{N_\phi} R_i)$, note that R_0 should be understood as containing the boundaries $\partial R_{i \neq 0}$. The gauge of $|\phi\rangle$ is such that $\phi_1(\mathbf{k}) > 0$ for $\mathbf{k} \in R_0$, denoted as $|\phi\rangle_{R_0}$, and $\phi_2(\mathbf{k}) > 0$ for $\mathbf{k} \in R_{i>0}$ (or any other smooth gauge), denoted as $|\phi\rangle_{R_i}$. At the boundaries between R_0 and $R_{i>0}$, one has the constituent condition

$$|\phi(\mathbf{k})\rangle_{R_0} = e^{i\gamma_{\mathbf{k}}^i} |\phi(\mathbf{k})\rangle_{R_i} \quad , \quad \mathbf{k} \in \partial R_i \quad , \quad (1)$$

where $\gamma_{\mathbf{k}}^i$ is the gauge mismatch of ϕ on the boundary of R_i . Since $\langle\phi(\mathbf{k})|\psi(\mathbf{k})\rangle \neq 0 \forall \mathbf{k}$, we can choose the gauge of ψ according to that of ϕ , such that their overlap is always real and positive,

$$R_i \langle\phi(\mathbf{k})|\psi(\mathbf{k})\rangle_{R_i} > 0 \quad , \quad \mathbf{k} \in R_i \quad , \quad i = 0, 1, 2, \dots, N_\phi \quad . \quad (2)$$

This endows ψ with the same constituent conditions at boundaries of $R_{i>0}$,

$$|\psi(\mathbf{k})\rangle_{R_0} = e^{i\gamma_{\mathbf{k}}^i} |\psi(\mathbf{k})\rangle_{R_i} \quad , \quad \mathbf{k} \in \partial R_i \quad . \quad (3)$$

The Chern number of ϕ is given by the total vorticities of the stitching phases γ^i [45, 49],

$$C_\phi = \sum_{i=1}^{N_\phi} v_i \quad , \quad v_i \equiv \oint_{\partial R_i} \frac{d\mathbf{k}}{2\pi} \cdot \nabla_{\mathbf{k}} \gamma_{\mathbf{k}}^i \quad . \quad (4)$$

Since ψ and ϕ share the same set of $\gamma_{\mathbf{k}}^i$, the two Chern numbers must be identical,

$$C_\psi = C_\phi \quad . \quad (5)$$

The proof of the first part is very similar. If $\langle\phi|\psi\rangle$ has $N_{\langle\phi|\psi\rangle}$ zeros, we instead partition the BZ into $N_\phi + N_{\langle\phi|\psi\rangle} + 1$ regions, where R_1, \dots, R_{N_ϕ} are defined the same as before, and one has in addition the regions $R_{N_\phi+j}$,

$j = 1, 2, \dots, N_{\langle\phi|\psi\rangle}$ surrounding nodes of $\langle\phi|\psi\rangle$. $R_0 = BZ \setminus (\cup_{i=1}^{N_\phi+N_{\langle\phi|\psi\rangle}} R_i)$. The gauge choice of ϕ remains the same as before. For ψ , one can still choose its gauge as $\langle\phi|\psi\rangle > 0$ in $R_0, R_1, \dots, R_{N_\phi}$. For the additional regions $R_{N_\phi+n}$, $n = 1, 2, \dots, N_{\langle\phi|\psi\rangle}$, one can choose any other smooth gauge, say, the component $\psi_1 > 0$, which induce $N_{\langle\phi|\psi\rangle}$ new stitching phases. The Chern number of ψ is the total vorticity of the $N_\phi + N_{\langle\phi|\psi\rangle}$ phases,

$$C_\psi = \sum_{i=1}^{N_\phi+N_{\langle\phi|\psi\rangle}} v_i = C_\phi + \sum_{i=N_\phi+1}^{N_\phi+N_{\langle\phi|\psi\rangle}} v_i, \quad (6)$$

where Eq. 4 is used to get the second equality. This implies that

$$\left| \sum_{i=N_\phi+1}^{N_\phi+N_{\langle\phi|\psi\rangle}} v_i \right| = |C_\psi - C_\phi|. \quad (7)$$

Note that the LHS of Eq. 7 satisfies $|\sum v_i| \leq \sum |v_i| \leq N_{\langle\phi|\psi\rangle}$, where we used $|v_i| = 0, \pm 1$, taking the viewpoint that vortices of vorticity $|v| > 1$ can be thought of as consisting of overlapping vortices of vorticity ± 1 . Thus

$$N_{\langle\phi|\psi\rangle} \geq |C_\psi - C_\phi|. \quad (8)$$

Theorem 2 *In 1D, the Berry phase γ of a real Bloch band, $|\psi(k)\rangle = (\psi_1(k), \psi_2(k), \dots)^t, \psi_a(k) \in \mathbb{R} \forall a$, is quantized to 0 or π . The overlap of two real bands $|\psi(k)\rangle$ and $|\phi(k)\rangle$, with Berry phases γ_ψ and γ_ϕ respectively, must have at least one node if $\gamma_\psi \neq \gamma_\phi$.*

Proof 2 Let us prove the first part first. The Berry phase of a band $|\psi(k)\rangle$ is defined as

$$\gamma = \int_0^{2\pi} dk \langle\psi(k)|i\partial_k\psi(k)\rangle \quad \text{mod } 2\pi. \quad (9)$$

Although this definition is not restricted to real bands, in our case, $|\psi(k)\rangle$ is a real band.

Assume the first component of ψ , $\psi_1(k)$, has N_ψ zeros at $k_1, k_2, \dots, k_{N_\psi}$. We fix the gauge of $|\psi(k)\rangle$ such that $\psi_1(k) > 0$ for $k \notin \{k_1, k_2, \dots, k_{N_\psi}\}$, and $\psi_2(k) > 0$ for $k \in \{k_1, k_2, \dots, k_{N_\psi}\}$. Under this gauge, the Berry phase accumulated within each nodeless segment $k : k_i + 0^+ \rightarrow k_{i+1} - 0^+$ vanishes. On the two sides of a nodal point k_i , however, the state $|\psi\rangle$ may differ by an overall sign, giving rise to a π Berry phase accretion across k_i . The total Berry phase γ_ψ is thus

$$e^{i\gamma_\psi} = \prod_{i=1}^{N_\psi} v_i, \quad v_i = \langle\psi(k_i - 0^+)|\psi(k_i + 0^+)\rangle = \pm 1. \quad (10)$$

This is the analogue of Eq. 4 of the 2D case. Thus the Berry phase γ_ψ is quantized to either 0 or π .

We note that the quantized Berry phase is equivalent to the Z_2 index introduced in Ref. 50.

Proof of the second part is very similar to the 2D case, where imposing $\langle\phi|\psi\rangle > 0$ induces a gauge for ϕ based on that of ψ . If the overlap of two real bands $\langle\phi(k)|\psi(k)\rangle$ has no nodes, then imposing $\langle\phi(k)|\psi(k)\rangle > 0$ everywhere enforces the sign changes of $|\phi(k)\rangle$ to be synchronized with those of $|\psi(k)\rangle$ at $\{k_1, k_2, \dots, k_{N_\psi}\}$, so they must have the same Berry phase. Thus if their Berry phases are different, there must exist node in their overlap.

A 1D 3-BAND MODEL WITH SYMMETRY-PROTECTED DQPT

To illustrate Thm.2, consider the following three band model in 1D,

$$H(k, t, m) = \begin{pmatrix} \sin k + m & \cos k + t & \\ \cos k + t & -\sin k & \cos k + t \\ & \cos k + t & \sin k - m \end{pmatrix}. \quad (11)$$

This model describes three coupled chains arranged as an $N \times 3$ square lattice, where N is the length of the chains along the x direction (assumed periodic), with horizontal (intra-chain nearest neighbor) and diagonal (next nearest

neighbor) hopping 1, vertical (inter-chain nearest neighbor) hopping $t \geq 0$, on-site mass modulation $m \geq 0$, and a π flux per square plaquette. Note that for $m = 0$ and when projected onto the subspace of the first two chains, $P = |1\rangle\langle 1| + |2\rangle\langle 2|$, the Hamiltonian reduces to $PH(k)P = \sin k \sigma_z + (\cos k + t)\sigma_x$, which, under the rotation $\sigma_z \rightarrow \sigma_y$, becomes the celebrated Su-Schrieffer-Heeger model. The central band always has Berry phase 0. For infinitesimal m , the topological transition occurs at $t \simeq 1$.

Since $H(k, t, m)$ is real, all three bands are subject to Thm. 2. For a fixed m , the top and bottom bands have Berry phase π if $H(k, t, m)$ is adiabatically connected with $H(k, t \rightarrow 0, m)$, or Berry phase 0 if $H(k, t, m)$ is adiabatically connected with $H(k, t \rightarrow \infty, m)$.

Berry phase for $m \rightarrow 0^+$

While the Hamiltonian Eq. 11 for generic t and m does not lend itself easily to closed-form diagonalization, the case with $m \rightarrow 0^+$ can be analytically solved. Topological classification of generic t and m can then be obtained, in principle, by adiabatic continuation (i.e. keeping both gaps open).

When $m = 0$, band degeneracy occurs at $k = \pm k_c$ if $t < 1$, with $k_c \geq 0$ determined by

$$\cos k_c + t = 0. \quad (12)$$

For $m \rightarrow 0^+$, one instead has two avoided crossings at $\pm k_c$.

Away from the avoided crossings, the eigenstates are given by those of $H(k, t, m = 0)$,

$$|\psi_k^\pm\rangle = \begin{pmatrix} \cos k + t \\ -\sin k \pm \sqrt{2(\cos k + t)^2 + \sin^2 k} \\ \cos k + t \end{pmatrix}, \quad |\psi_k^3\rangle = \begin{pmatrix} 1 \\ 0 \\ -1 \end{pmatrix}, \quad (13)$$

$$E_k^\pm = \pm \sqrt{2(\cos k + t)^2 + \sin^2 k}, \quad E_k^3 = \sin k. \quad (14)$$

Note that the eigenstates are *un-normalized*. E^\pm and E^3 are the corresponding eigenvalues. Close to, but not at, the avoided crossings, one can write $k = \pm k_c + \delta$ and expand ψ^\pm to first order of δ ,

$$|\psi_{k_c+\delta}^+\rangle = -\sin k_c \delta \begin{pmatrix} 1 \\ 0 \\ 1 \end{pmatrix} + \mathcal{O}(\delta^2), \quad |\psi_{k_c+\delta}^-\rangle = -2 \sin k_c \begin{pmatrix} 0 \\ 1 \\ 0 \end{pmatrix} - \delta \begin{pmatrix} \sin k_c \\ 2 \cos k_c \\ \sin k_c \end{pmatrix} + \mathcal{O}(\delta^2), \quad (15)$$

$$|\psi_{-k_c+\delta}^+\rangle = 2 \sin k_c \begin{pmatrix} 0 \\ 1 \\ 0 \end{pmatrix} + \delta \begin{pmatrix} \sin k_c \\ -2 \cos k_c \\ \sin k_c \end{pmatrix} + \mathcal{O}(\delta^2), \quad |\psi_{-k_c+\delta}^-\rangle = \sin k_c \delta \begin{pmatrix} 1 \\ 0 \\ 1 \end{pmatrix} + \mathcal{O}(\delta^2). \quad (16)$$

While the un-normalized ψ^\pm are smooth over the entire BZ, their normalized versions would experience a phase (i.e. gauge) mismatch near the avoided crossings, which gives rise to Berry phase. Consider, for example, the Berry phase of ψ^+ . From the first equation in Eq. 15, the normalized ψ^+ is $|\tilde{\psi}_{k_c+\delta}^+\rangle = -\text{Sgn}(\delta) \begin{pmatrix} 1 \\ 0 \\ 1 \end{pmatrix} / \sqrt{2}$. It picks up an overall negative sign going from $k_c - 0^+$ to $k_c + 0^+$, i.e. a π Berry phase change. Anywhere else its gauge is smooth, therefore ψ^+ has a π Berry phase.

Similar analysis shows that ψ^- acquires a π Berry phase passing through $-k_c$.

For $t > 1$, $\cos k + t$ never reaches zero, hence ψ^\pm both have a smooth and periodic gauge and therefore their Berry phases are zero.

The Berry phase of the central band is always zero for any t as $|\psi_k^3\rangle$ is k -independent. This is consistent with the fact that the total Berry phase of all bands (for any band models) is always zero.

DQPT in quench from topological to trivial phase

We prepare the pre-quench state by filling the lowest band in the topological phase $H_I(k) = H(k, t \rightarrow 0, m)$,

$$|\Psi\rangle = \prod_k (\psi_k^-)^\dagger |\emptyset\rangle. \quad (17)$$

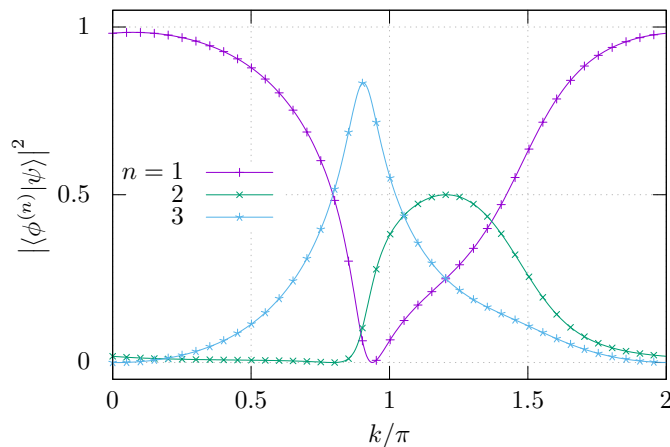


FIG. 1. Overlap between pre-quench band and post-quench eigenstates for the 3-band model Eq. 11. Pre-quench parameters are $t_i = 0.8, m_i = 0.5$. Its lowest band has Berry phase π and is used as the pre-quench state. Post-quench Hamiltonian is the $t_f \rightarrow \infty$ limit (cf. Eq. 18), all eigenstates $\phi^{(1,2,3)}$ there have 0 Berry phase. According to Thm. 2, all three overlaps must have nodes, which can be verified from the plot. The DQPT condition $\exists k : |\langle \phi^{(n)}(k) | \psi(k) \rangle|^2 \leq \frac{1}{2} \forall n$ is thus protected.

At time $t = 0$, we switch the Hamiltonian to the following topologically trivial one,

$$H_F(k) = H(k, t = t_F \rightarrow \infty, m) = t_F \begin{pmatrix} 0 & 1 & 0 \\ 1 & 0 & 1 \\ 0 & 1 & 0 \end{pmatrix}. \quad (18)$$

Its eigenstates and eigenvalues are

$$|\phi_k^\pm\rangle = \frac{1}{2} \begin{pmatrix} 1 \\ \pm\sqrt{2} \\ 1 \end{pmatrix}, \quad |\phi_k^3\rangle = \frac{1}{\sqrt{2}} \begin{pmatrix} 1 \\ 0 \\ -1 \end{pmatrix}, \quad E_k^\pm = \pm\sqrt{2}t_F, \quad E_k^3 = 0. \quad (19)$$

Fig. 1 plots the overlap of the pre-quench band with all three post-quench eigenstates, verifying that all three overlaps have node as required by Thm. 2. These nodes in turn guarantees the DQPT condition $\exists k : |\langle \phi^{(n)}(k) | \psi(k) \rangle|^2 \leq \frac{1}{2} \forall n$.

GENERALIZED HOFSTADTER MODEL

A generalization of the q -band Hofstadter model is

$$H(k_x, k_y, p, q, t, m) = \begin{pmatrix} d_1 & v_1 & & & v_q e^{ik_y} \\ v_1 & d_2 & v_2 & & \\ & & v_2 & \ddots & \\ & & & \ddots & \ddots \\ v_q e^{-ik_y} & & & & v_{q-1} \\ & & & & v_{q-1} & d_q \end{pmatrix}, \quad (20)$$

$$d_a = 2 \cos(k_x + a\phi) + a m, \quad v_a = 1 + 2t \cos \left[k_x + \left(a + \frac{1}{2} \right) \phi \right], \quad a = 1, 2, \dots, q, \quad \phi = 2\pi \frac{p}{q}. \quad (21)$$

Here p and q are co-prime integers, ϕ is the flux per square plaquette, the magnetic unit cell is chosen along the y direction, t is the amplitude of the second neighbor hopping (with nearest neighbor hopping set to 1). The Pierls phases along the diagonals (i.e. of the second neighbor hops) are chosen so that the flux per triangle is $\phi/2$. Note that for $q = 2$, the off-diagonal matrix element is $v_1 + v_q e^{ik_y}$. We also impose a sawtooth potential in the y -direction, $V_y = (y \bmod q) \times m$, which is commensurate with the magnetic unit cell.

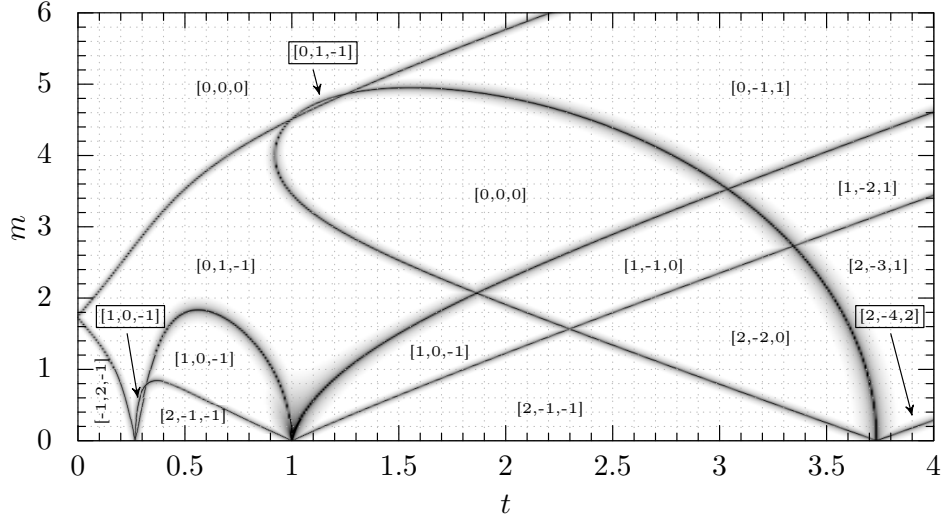


FIG. 2. Topological phase diagram of the 3-band Hofstadter model in the $t-m$ space. Black lines are phase boundaries (where at least one of the two spectral gaps collapses). Unboxed labels denote the Chern numbers (from lower to higher energy bands) of the corresponding phases. Boxed labels denote the Chern numbers in the phase indicated by the arrows. Only $t \geq 0$ and $m \geq 0$ are shown, other quadrants can be obtained by its mirror image, which follows from (1) that the Chern numbers remain the same for $m \rightarrow -m$, and (2) that the Chern numbers reverse order for $t \rightarrow -t$.

Phase diagram

The 3-band model used in the text amounts to fixing $p = 1, q = 3$. Fig. 2 shows its topological phase diagram in the $t-m$ plane. We only plot the $t \geq 0$ and $m \geq 0$ quadrant, the other three quadrants can be obtained by taking its mirror image, noting that (1) the Chern numbers remain the same for $m \rightarrow -m$, and that (2) the Chern numbers reverse order for $t \rightarrow -t$.

Protected vs unprotected DQPT

While the DQPT amplitude condition only require the existence of at least one \mathbf{k} point at which all overlaps $|\langle \phi^{(n)}(\mathbf{k}) | \psi(\mathbf{k}) \rangle|^2 \leq \frac{1}{2} \forall n$, it is not a phase-robust feature. This is illustrated in Panels (a) and (b) in Fig. 3, where both are in the same pre- and post-quench topological phases, yet simply by tuning the post-quench parameter t_f the DQPT in (b) can be avoided. Therefore, a protected DQPT requires the existence of \mathbf{k} -space nodes in all overlaps, which would guarantee the amplitude condition. This is demonstrated in Fig. 3 (c).

Detailed analysis of Fig. (2) in text

Here we analyze all quench types shown in Fig. 2 in the main text, reproduced here in Fig. 4 for convenience.

There are 18 quench types shown in Fig. 4 (3 pre-quench bands, 6 post-quench phases). Their relation with DQPT is summarized in the table below,

	1	2	3	4	5	6	
	[0,0,0]	[0,1,-1]	[0,0,0]	[1,-1,0]	[1,-2,1]	[2,-3,1]	
$\psi^{(1)} (C = 1)$	Y	A	Y	X	N	A), (22)
$\psi^{(2)} (C = -1)$	Y	S	Y	X	Y	Y	
$\psi^{(3)} (C = 0)$	S	S	N	X	Y	Y	

where we have

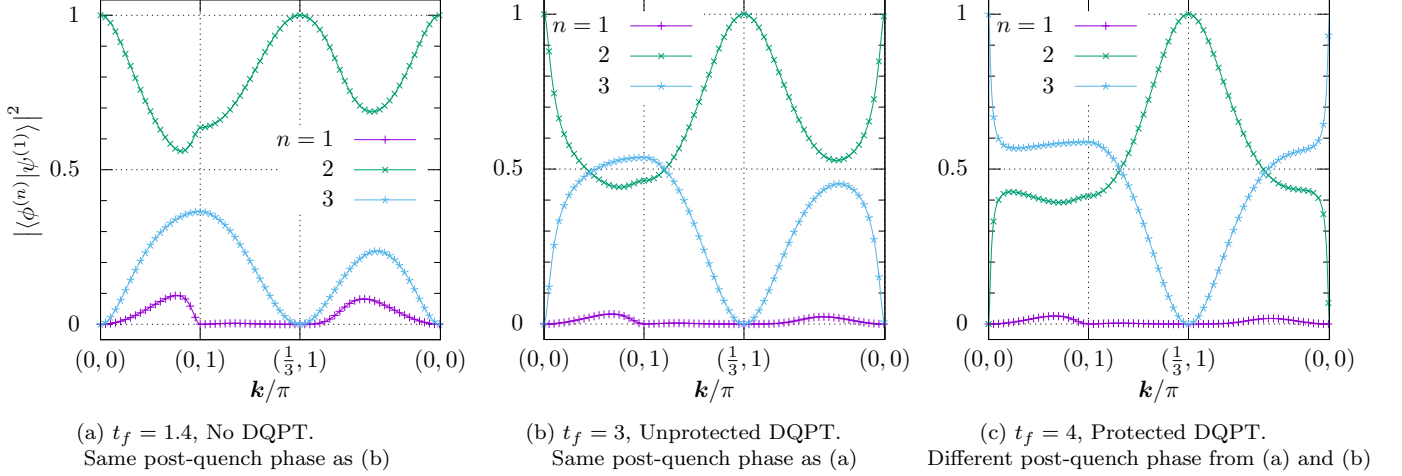


FIG. 3. Protected vs unprotected DQPT of the 3-band generalized Hofstadter model. In all three panels, we fix the pre-quench Hamiltonian H_I with $t_i = -0.8, m_i = 0$, and use three different t_f , as shown in panel captions, for the post-quench Hamiltonian, while keeping $m_f = 0$. H_I is in the topological phase with Chern numbers $[-1, -1, 2]$ for its three bands. For panels (a) and (b), H_F is in the phase $[2, -1, -1]$, and for panel (c), it is in phase $[2, -4, 2]$. We plot the overlap of $\psi^{(1)}$ with $\phi^{(1,2,3)}$ along high symmetry lines (on which overlap minima will occur because we have set $m_i = m_f = 0$). Panel (b) illustrates unprotected crossing of $n = 2$ and 3 near $\frac{1}{2}$, at which point the DQPT amplitude condition $|\langle \phi^{(n)}(\mathbf{k}) | \psi^{(1)}(\mathbf{k}) \rangle|^2 \leq \frac{1}{2} \forall n$ is satisfied, yet since the $n = 2$ line (green line with cross) never reaches zero, this crossing is not robust, and can be removed by tuning H_I and H_F within their respective phases. This type of avoided crossing is shown in (a), note that in this case the $n = 2$ line lies entirely above $\frac{1}{2}$, hence DQPT is forbidden. In (c), all overlaps touch zero, thus the crossing near $\frac{1}{2}$ and DQPT is robust.

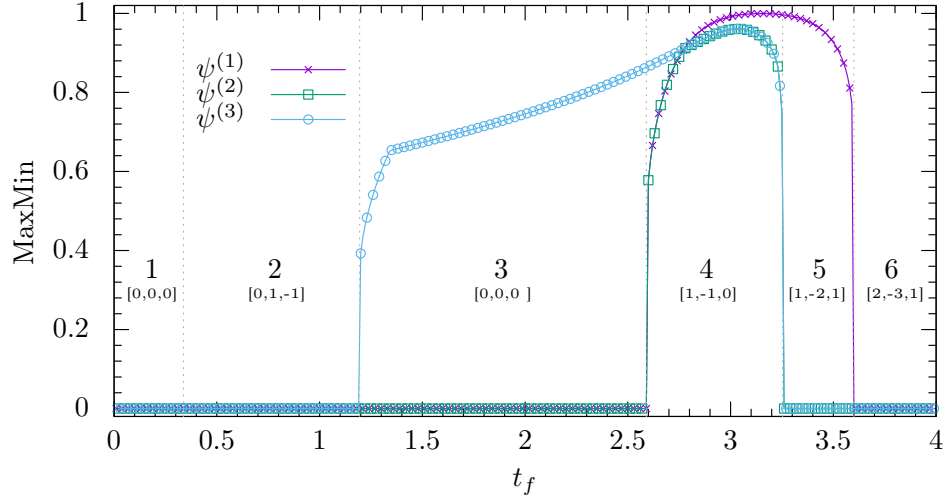


FIG. 4. (Color online) Plot of ψ_{MaxMin} (see main text for definition) as functions of the post-quench t . Pre-quench state is prepared by filling one of the three bands $\psi^{(1,2,3)}$ of the 3-band generalized Hofstadter model with parameters $t_i = 3$ and $m_i = 2.8$. Post-quench $H(\mathbf{k})$ has fixed $m_f = 3$ and a varying t_f , sweeping it through six topological phases labeled by its three Chern numbers (ordered from lower to higher band). The pre-quench Hamiltonian is in phase 4. A robust DQPT can be identified by $\psi_{\text{MaxMin}} = 0$ (see main text). Note that ψ_{MaxMin} changes between zero and non-zero only at phase boundaries, verifying robust DQPT as a feature of topological phases insensitive to parameter tuning.

- *Topological DQPT*: 8 entries with “Y”. As discussed in the main text, these are quenches with DQPT due to all post-quench Chern numbers being different from the Chern number of the pre-quench band. Thm. 1 then guarantees the overlap nodes.
- *Symmetry protected DQPT*: 3 entries with “S”. As discussed in the main text, these are quenches where at least one of the post-quench Chern number is identical to that of the pre-quench band, yet on high symmetry lines

$k_y = 0$ and π , their overlap still exhibits nodes protected by Berry phase. This subclass will be discussed in detail in the next section.

- 3 entries with “X”, which denote quenches with no robust DQPT because the pre-quench and post-quench Hamiltonians are in the same topological phase.
- 2 entries with “N”, which denote quenches with no robust DQPT, because the topological transition between the pre-quench and post-quench Hamiltonians only involves collapsing a gap which is not immediate to the pre-quench band (i.e., the pre-quench band never touches other bands over the topological transition). For example, when quenching the lowest band $\psi^{(1)}$ toward phase 5 (with final states $\phi^{1,2,3}$), $\psi^{(1)}$ and $\phi^{(1)}$ are adiabatically related (i.e. without collapsing the lowest spectral gap in $H(\mathbf{k})$), hence it is understandable that there is no node in their overlap, which precludes a robust DQPT.
- 2 entries with “A”. As discussed in the main text, these quenches exhibit an even number of overlap nodes at $k_y = 0$ and/or π , but these nodes cannot be accounted for by Thms. 1 and 2 (see Eq. 23 for Berry phases). By tuning $t_{i,f}$ and $m_{i,f}$, we were able to shift the nodes along k_x as well as to change the total number of nodes by an even number, but could not entirely eliminate them. We suspect however that they could eventually be eliminated in an enlarged parameter space

Symmetry-protected DQPT

There are three entries in Eq. 22 (see also Fig. 4) where the occurrence of DQPT is due to symmetry protection. For example, consider the quench from the highest band $|\psi^{(3)}\rangle$ of phase 4 toward phase 1. The Chern number of the pre-quench band and all three post-quench bands are 0, thus there is no node protected by Thm. 1. However, since $H(k_x, -k_y) = H(k_x, k_y)^*$, the eigenstates of H at $k_y = 0$ and π are real, and can hence be classified by their respective Berry phases over the k_x loop. Numerically one finds the Berry phases to be

$$\begin{array}{c|cccccc}
 & 1 & 2 & 3 & 4 & 5 & 6 \\
 \hline
 \psi^{(1)} & 0, 0 & 0, 0 & 0, 0 & 0, \pi & 0, \pi & \pi, \pi \\
 \psi^{(2)} & 0, 0 & 0, \pi & \pi, \pi & \pi, 0 & 0, 0 & \pi, 0 \\
 \psi^{(3)} & 0, 0 & 0, \pi & \pi, \pi & \pi, \pi & 0, \pi & 0, \pi
 \end{array} \quad , \quad (23)$$

where the ordered number pair in each cell denotes the Berry phases at $k_y = 0$ and π , respectively, of a state (row) in a topological phase (column). In Fig. 4, the pre-quench Hamiltonian is in phase 4, where the two Berry phases of $\psi^{(3)}$ are both π , whereas those of the post-quench states (phase 1) are all zero. Thus while $\psi^{(3)}$ as well as $\phi^{1,2,3}$ are all trivial in the quantum Hall sense, they nonetheless belong to different classes at the high symmetry k_y 's, hence the nodes in their overlaps are protected by Thm. 2, leading to a protected DQPT.